

179 (1974).

⁶R. A. Cowley, Phys. Rev. B **13**, 4877 (1976).

⁷E. Courtens, Phys. Rev. Lett. **41**, 17 (1978). The same crystal was used here.

⁸As predicted by E. Pytte and H. Thomas, Solid State Commun. **11**, 161 (1972), and as observed in the FE phase by M. D. Mermelstein and H. Z. Cummins, Phys. Rev. B **16**, 2177 (1977).

⁹See Pytte and Thomas, Ref. 8.

¹⁰F. Jona and G. Shirane, Ref. 4; $\alpha = 3.84 \times 10^{12}$, $\beta = 2.9 \times 10^{-12}$, and $b = 5.0 \times 10^{-7}$, in cgs units.

¹¹E. Courtens, R. Gammon, and S. Alexander, to be published.

¹²S. Haussühl, Z. Kristallogr., Kristallgeom., Kristallphys., Kristallchem. **120**, 401 (1964).

¹³Symmetry-breaking continuous elastic transitions always have a soft elastic wave as shown by S. Aubry and R. Pick, J. Phys. (Paris) **32**, 657 (1971).

¹⁴H. Wagner and H. Horner, Adv. Phys. **23**, 587 (1974).

¹⁵R. L. Melcher, G. Guntherodt, T. Penney and F. Holtzberg, IEEE Trans. Sonics Ultrason. **23**, 205 (1976).

Vacancies and the Chemical Trapping of Hydrogen in Silicon

H. J. Stein

Sandia Laboratories, Albuquerque, New Mexico 87185

(Received 9 July 1979)

The first evidence for SiH₁-like centers in crystalline Si (*c*-Si) is presented from infrared measurements of H (D) implanted at 80 K. In contrast to SiH₁ centers in amorphous Si (*a*-Si) which are stable to ≈ 700 K, the crystalline band anneals below 300 K with an activation energy and illumination enhancement that are characteristic of the Si vacancy. These results relate specific defects for implanted H in *c*-Si to previous observations for H in *a*-Si.

Hydrogen bonds chemically in both crystalline Si (*c*-Si)^{1,2} and amorphous Si (*a*-Si)³ and produces significant changes in electrical properties.⁴ There is, however, little understanding of structural changes which accompany hydrogenation of Si. Understanding the relationships between structural composition and chemical bonding of hydrogen in Si is a necessary part of understanding electrical properties of hydrogenated Si. Hydrogen implantation into *c*-Si at 300 K produces a complex SiH stretch-frequency spectrum of at least twelve infrared absorption bands.^{1,2} Because these absorption bands have different annealing characteristics,^{1,2} they represent discrete SiH centers. However, since nuclear reaction-channeling analysis⁵ shows that a major fraction of hydrogen implanted into *c*-Si at 300 K occupies a well-defined crystalline interstitial site, it was suggested^{1,5} that the many SiH stretch frequencies in implanted *c*-Si are associated with different atomic-displacement-produced defects surrounding a well-defined interstitial hydrogen position within the crystalline lattice.⁵ In contrast to the many SiH bands produced by H implantation into *c*-Si at 300 K, implantation into *a*-Si yields a single broad band⁶ which has been assigned to the one-hydrogen (SiH₁) center.³

Reported herein are results obtained from studies on SiH stretch frequencies for hydrogen implanted into crystalline Si at low temperature. From these results one can infer that low-temperature. From these results one can infer that low-temperature H implantation into *c*-Si produces Si-H bonding similar to the SiH₁ bonding observed in *a*-Si. In addition, from the annealing studies reported here, one can relate the loss of this band to the motion of the Si vacancy in *c*-Si.

Hydrogen implantations of 6×10^{15} cm⁻² were made at 50 and 100 keV at 80 K into both 0.63 \times 1.27 cm² faces of high-resistivity (111) samples of *n*-type crucible-grown Si. The penetration depth for 100-keV hydrogen into Si is 1 μ m; therefore, the average concentration within an implanted layer is $\sim 1.2 \times 10^{20}$ H/cm³.

The solid trace in Fig. 1 shows the SiH absorption spectrum produced by H implantation into *c*-Si at 80 K. This spectrum is much less complex than that for implantation at 300 K. The major SiH stretch frequency at 1990 cm⁻¹ observed after low-temperature implantation of hydrogen into⁷ *c*-Si is essentially the same as that for the SiH₁ centers produced by implantation into *a*-Si at 300 K (dotted trace of Fig. 1). An

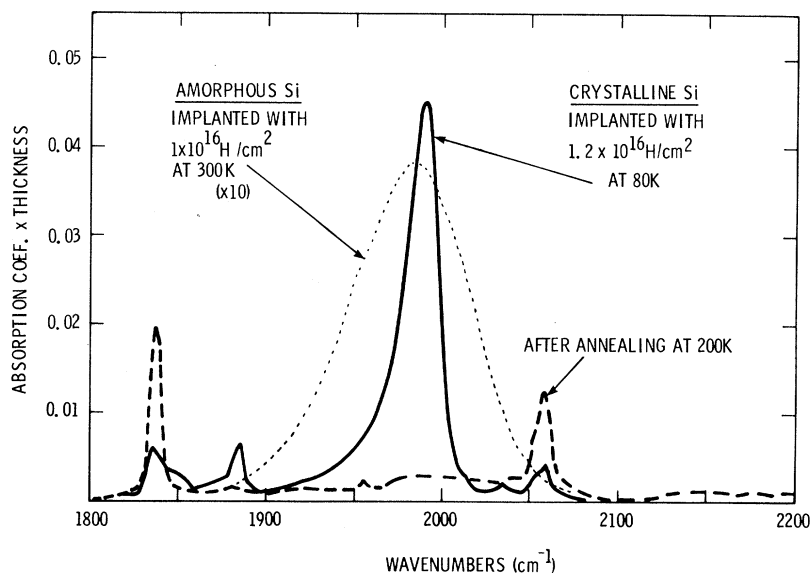


FIG. 1. SiH stretch frequencies produced by hydrogen implantation into crystalline Si at 80 K (solid line), and after annealing at 200 K (dashed line). Also shown are results from hydrogen-implanted amorphous Si (dotted line) at 300 K. Absorption and atom fluences are expressed per implanted layer.

implantation of 100-keV deuterium into *c*-Si produced a similar center, but the stretch frequency was shifted to 1440 cm^{-1} as expected, because of the mass difference between hydrogen and deuterium. Bombardment with He produced neither the 1990-cm^{-1} nor the 1440-cm^{-1} band which further confirms assignment of the 1990-cm^{-1} band to an SiH center.

The peak absorption coefficient multiplied by the full width at half maximum divided by the implanted H atoms/cm² is ~ 3 times larger for the 1990-cm^{-1} band in *c*-Si than for the SiH₁ band in *a*-Si. This difference indicates that hydrogen implanted into *c*-Si at 80 K is effectively trapped, and the resultant SiH center has an even larger oscillator strength than that for SiH₁ centers in *a*-Si. The 1990-cm^{-1} band in *c*-Si and a weaker band at 1885 cm^{-1} disappear upon annealing at 200 K while the intensities of bands at 1840 and 2060 cm^{-1} increase. This annealing of the 1990-cm^{-1} band from *c*-Si at 200 K, as shown by the dashed line in Fig. 1, contrasts sharply with the SiH₁ band in *a*-Si which is stable to $\sim 400^\circ\text{C}$.

To more fully characterize the annealing processes for the 1990-cm^{-1} band, isothermal annealing measurements were made at 130, 140, 150, and 160 K. An activation energy for the annealing process was obtained by plotting the natural logarithm of the time for one-half the centers to anneal versus inverse annealing temperature as

shown in Fig. 2. Absorption measurements were made at 80 K after selected times at the annealing temperature. Also plotted in Fig. 2 are data for neutral-vacancy annealing obtained by Watkins⁸ from EPR studies of pulled and float-zone Si.

Because the activation energy of $0.34 \pm 0.03\text{ eV}$ obtained in the present study agrees closely with that obtained by Watkins for neutral-vacancy annealing,⁸ one can infer that vacancy motion probably controls the annealing of the 1990-cm^{-1} band. The shorter half-lives for vacancies in pulled than in float-zone Si are explained by vacancy trapping at oxygen which is present in higher concentrations in pulled than in float-zone Si. Ion bombardment creates high concentrations of sinks for mobile defects⁹ which accounts for the shorter half-lives observed in the present experiment than for those in the EPR study of neutral vacancy annealing in electron-bombarded *c*-Si. Kinetics for vacancy annealing in the present study are more complex than the first-order kinetics reported by Watkins for randomly distributed vacancies produced by electron bombardment.⁸ Such complex annealing kinetics are typical of defects produced by neutron and ion bombardment of Si.⁹

Since vacancy annealing is charge-state dependent,⁸ illumination with photons of $E > 1.1\text{ eV}$ should produce hole-electron pairs and the re-

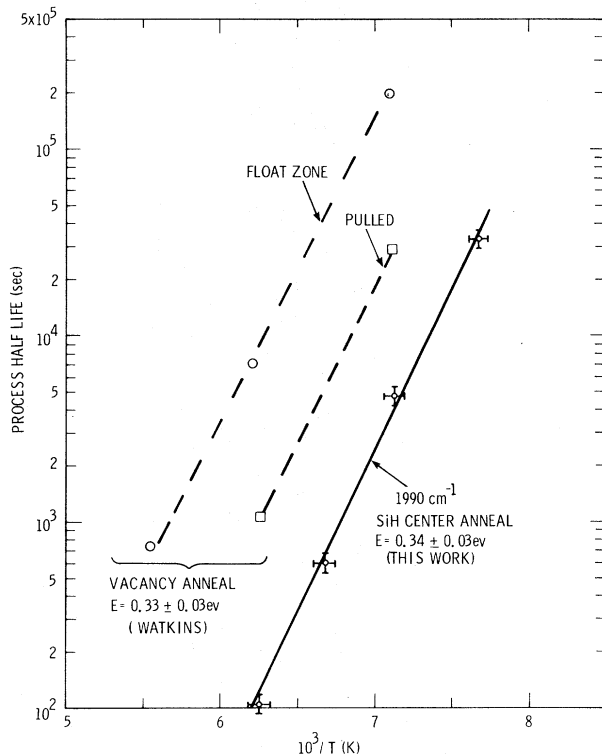


FIG. 2. Activation energy for annealing of the 1990-cm^{-1} SiH band in crystalline Si (solid line), and for annealing of neutral vacancies (dashed lines, Watkins, Ref. 8) in Si.

sultant negative charge state at 80 K for a fraction of the vacancies should induce annealing.⁸ Indeed, 1-hr exposure of implanted layers to a 1-W filtered-output xenon lamp ($E_{\text{photon}} \leq 3.9$ eV) produced 75% annealing of the 1990-cm^{-1} band. The sample-block temperature increased by 3 K during illumination. This temperature increase is insufficient to cause annealing of neutral vacancies, and the temperature difference between the two sides of the sample resulting from the energy input on one surface was estimated to be < 0.1 K. For additional assurance that annealing is light induced rather than thermally induced, the 1990-cm^{-1} band was produced by implanting only one surface at 80 K. The sample surface opposite the implanted layer was exposed for 1 hr to illumination from the xenon lamp. In this case the unimplanted side of the sample acted as a band-gap filter, and no annealing occurred within an experimental uncertainty of 10%. The sample was then rotated to expose the implanted layer to illumination and annealing was observed. Thus, both the thermally induced and photoin-

duced annealings of the 1990-cm^{-1} -SiH band in *c*-Si correspond to a vacancy-controlled mechanism and demonstrate interaction between SiH centers and vacancies in Si. Vacancy motion, which is a characteristic of *c*-Si, is also evidence that the implanted layer remains crystalline.

Four possibilities have been considered to explain changes in the SiH-defect centers induced by annealing, under tacit assumptions that a defect is required for the chemical trapping of hydrogen in Si and that the SiH center itself is immobile: (a) motion of vacancies away from SiH-vacancy centers; (b) motion of free vacancies to SiH-vacancy centers; (c) motion of free vacancies to SiH-interstitial Si centers; and (d) motion of vacancies away from SiH-vacancy clusters. Explanation (d) is favored over the other three primarily because EPR studies by Brower¹⁰ on low-temperature neutron-irradiated Si showed the formation of distorted four-vacancy centers (clusters) rather than isolated vacancies. The hypothesis that hydrogen is trapped at vacancy clusters in *c*-Si after low-temperature implantation is supported by the similarity of the SiH frequency in this material to the SiH₁ frequency for hydrogen associated with voids in *a*-Si.

In summary the results obtained in the present study demonstrate interactions between vacancies and SiH centers in *c*-Si, and relate an SiH center in *c*-Si to SiH₁ centers in *a*-Si. Additional studies such as EPR and channeling/backscattering are needed to further delineate the SiH centers responsible for the 1990-cm^{-1} band in *c*-Si.

The author is indebted to P. S. Peercy and F. L. Vook for helpful discussions on the manuscript, and to R. H. Baxter for assistance with the measurements. This work was sponsored by the U. S. Department of Energy, Office of Basic Energy Sciences, under Contract No. DE-AC04-76-DP00789. Sandia Laboratories is a U. S. Department of Energy facility.

¹H. J. Stein, J. Electr. Mater. **4**, 159 (1975).

²N. N. Gerasimenko, M. Rolle, Li-Jen Cheng, Y. H. Lee, J. C. Corelli, and J. W. Corbett, Phys. Status Solidi (b) **90**, 689 (1978).

³M. H. Brodsky, M. Cordona, and J. J. Cuomo, Phys. Rev. B **16**, 3556 (1977).

⁴W. E. Spear and P. G. LeComber, Philos. Mag. **33**, 935 (1976); Y. Ohmura, Y. Zohta, and M. Kanazawa, Solid State Commun. **11**, 263 (1972).

⁵S. T. Picraux and F. L. Vook, *Phys. Rev. B* **18**, 2066 (1978); S. T. Picraux, F. L. Vook, and H. J. Stein, in *Proceedings of the International Conference on Defects and Radiation Effects in Semiconductors*, Nice, France, September 1978 (to be published).

⁶H. J. Stein and P. S. Peercy, *Appl. Phys. Lett.* **34**, 604 (1979).

⁷Presented in brief by H. J. Stein, *Bull. Am. Phys. Soc.* **24**, 435 (1979).

⁸G. D. Watkins, *J. Phys. Soc. Jpn.* **18**, 22 (1963), and *Radiation Damage in Semiconductors* (Academic, New York, 1965), p. 97.

⁹H. J. Stein, in *Radiation Effects in Semiconductors*, edited by J. W. Corbett and G. D. Watkins (Gordon and Breach, New York, 1979), p. 125.

¹⁰K. L. Brower, in *Ion Implantation in Semiconductors*, edited by F. Chernow, J. A. Borders, and D. K. Brice (Plenum, New York, 1976), p. 427.

Observation of Singular Behavior in the Focusing of Ballistic Phonons in Ge

J. C. Hensel and R. C. Dynes

Bell Laboratories, Murray Hill, New Jersey 07974

(Received 3 August 1979)

High-resolution heat-pulse experiments reveal that transverse, ballistic phonons in Ge are focused into sharply defined beams along the [001] and [110] axes. Angular distributions within these beams display fine-structure representing focusing singularities. It is shown that these features are dependent in a sensitive way on the topology of the phonon-frequency surface.

In pure crystalline dielectric solids at low temperatures the propagation of high-frequency acoustic phonons is ballistic in nature.¹ Elastic anisotropy of the solid imparts directional characteristics to the ballistic propagation—an effect called “phonon focusing.”^{2,3} In a heat-pulse experiment in Ge distinguished by high angular resolution and wide angular coverage we have discovered a number of remarkable features in the focusing patterns quite unlike anything reported heretofore, *viz*: (1) the transverse acoustical (TA) phonons preferentially radiate in very strong, but narrow (a few degrees width) and sharply defined beams centered on the crystallographic axes [001] and [110]; (2) within these focusing “cones” there appear even sharper spikes representing focusing singularities. In this Letter we show that these observations lead to new insights into the physics of phonon propagation. Besides their obvious relevance to phonon optics,⁴ high-frequency phonon generation and propagation, Kapitza resistance,¹ and low-temperature thermal conductivity,⁵ these developments are particularly timely since it appears that the strong directionality of phonon focusing is partly responsible (via the phonon wind mechanism^{6,7}) for the highly anisotropic shape of the electron-hole droplet cloud, a matter currently being investigated intensively.

Basically, phonon focusing, the concentration of phonon flux along certain directions, depends

upon the fact that in anisotropic medium the direction of energy propagation, given by the group velocity vector \vec{v}_g , does not necessarily coincide with the phase velocity \vec{v}_p , a vector parallel to the phonon wave vector \vec{k} . Since the direction of \vec{v}_g is given by the normal to the constant-frequency surface (ω surface), focusing will arise when, as a result of elastic anisotropy, the surface departs from a spherical shape—an extreme but simple example being a cube for which phonon intensity is finite only for directions parallel to the cubic axes and zero otherwise. Obviously focusing effects will be quite sensitive to details of the ω surface as we shall demonstrate.

The experiments were performed in liquid He II at ~ 1.8 K and can be visualized from the inset in Fig. 1. The sample, in the shape of a hemicylinder, can be rotated about its axis by means of a shaft connected to a goniometer at the top of the cryostat. Heat pulses are generated optically by a Q-switched yttrium aluminum garnet laser (pulse width 150 nsec) beam focused on the cylindrical surface which is cylindrical surface which is coated with an evaporated Constantan film. Power densities were kept low, ≈ 1 W/mm², to avoid formation of a hot spot.⁷ The detector is a thin-film granular Al superconducting bolometer in the form of a narrow stripe aligned with the axis of rotation. Its dimensions, 0.1 mm wide by 1.0 mm long, define the overall angular resolution for the experiment: $\pm 2.9^\circ$ in vertical